JOURNAL OF GEOPHYSICAL RESEARCH, VOL. 103, NO. D23, PAGES 31,203–31,216, DECEMBER 20, 1998

Vertical distributions of lightning NO_x for use in regional and global chemical transport models

Kenneth E. Pickering,[1] Yansen Wang,[2] Wei-Kuo Tao,[3]
Colin Price,[4] and Jean-Francois Müller[5]

Abstract. We have constructed profiles of lightning NO_x mass distribution for use in specifying the effective lightning NO_x source in global and regional chemical transport models. The profiles have been estimated for midlatitude continental, tropical continental, and tropical marine regimes based on profiles computed for individual storms in each regime. In order to construct these profiles we have developed a parameterization for lightning occurrence, lightning type, flash placement, and NO_x production in a cloud-scale tracer transport model using variables computed in the two-dimensional Goddard Cumulus Ensemble (GCE) model. Wind fields from the GCE model are used to redistribute the lightning NO_x throughout the duration of the storm. Our method produces reasonable results in terms of computed flash rates and NO_x mixing ratios compared with observations. The profiles for each storm are computed by integrating the lightning NO_x mass across the cloud model domain for each model layer at the end of the storm. The results for all three regimes show a maximum in the mass profile in the upper troposphere, usually within 2–4 km of the tropopause. Downdrafts appear to be the strongest in the simulated midlatitude continental systems, evidenced by substantial lightning NO_x mass (up to 23%) in the lowest kilometer. Tropical systems, particularly those over marine areas, tended to have a greater fraction of intracloud flashes and weaker downdrafts, causing only minor amounts of NO_x to remain in the boundary layer following a storm. Minima appear in the profiles typically in the 2–5 km layer. Even though a substantial portion of the NO_x is produced by cloud-to-ground flashes in the lowest 6 km, at the end of the storm most of the NO_x is in the upper troposphere (55–75% above 8 km) in agreement with observations. With most of the effective lightning NO_x source in the upper troposphere where the NO_x lifetime is several days, substantial photochemical O_3 production is expected in this layer downstream of regions of deep convection containing lightning. We demonstrate that the effect on upper tropospheric NO_x and O_3 is substantial when the vertical distribution of the lightning NO_x source in a global model is changed from uniform to being specified by our profiles. Uncertainties in a number of aspects of our parameterization are discussed.

1. Introduction

Three-dimensional regional and global chemical transport models (CTMs) are increasingly being used in atmospheric chemistry research and in assessment of the effects of anthropogenic activities. Model simulation of full tropospheric ozone chemistry requires detailed specification of all major NO_x sources (fossil fuel combustion at the surface, biomass burning, soil emission, influx from the stratosphere, aircraft, and lightning). Considerable work has been done to develop detailed surface-source inventories [e.g., *Benkovitz et al.*, 1996] and aircraft emission patterns [*Baughcum et al.*, 1996]. NO_x from lightning remains the source with the largest uncertainty. Global source strength estimates range from 2 to over 200 Tg N yr^{-1}, although the 2–10 Tg N yr^{-1} range appears to be more realistic for balancing the nitrogen budget according to recent CTM experiments [e.g., *Levy et al.*, 1996; *Y. Wang et al.*, 1998]. The information concerning the lightning source that is required for three-dimensional (3-D) modeling includes the geographic distribution of lightning flashes by month, the NO_x production per flash, and the vertical distribution of the resulting NO_x as redistributed by a convective storm. In this paper we focus on the development of parameterizations for the vertical distribution of lightning NO_x for use in 3-D models. Some global models (e.g., the IMAGES model [*Müller and Brasseur*, 1995]) using a global annual lightning NO_x source strength of 5 Tg N yr^{-1} have shown lightning to be the largest contributor to upper tropospheric NO_x at all latitudes and in all seasons [*Lamarque et al.*, 1996]. Therefore, in order to evaluate the relative impacts of the various NO_x sources on upper tropospheric photochemistry, proper specification of the effective vertical profile of the lightning NO_x source is a high priority.

Ideally, CTMs should have convective parameterization schemes that are sufficiently accurate in predicting the location and transport features of deep convective events such that

[1]Joint Center for Earth System Science, Department of Meteorology, University of Maryland, College Park.
[2]Science, Systems, and Applications, Inc., Greenbelt, Maryland.
[3]NASA Goddard Space Flight Center, Greenbelt, Maryland.
[4]Department of Geophysics and Planetary Science, Tel Aviv University, Ramat Aviv, Israel.
[5]Belgian Institute for Space Aeronomy, Brussels, Belgium.

Paper number 98JD02651.
0148-0227/98/98JD-02651$09.00

lightning flashes could be placed at these locations and the subgrid vertical transport be allowed to vertically redistribute the lightning NO_x. More accurate representation of the geographic distribution of lightning is typically obtained from global lightning climatologies, but when such climatologies are used in a CTM, lightning NO_x production is not consistent with the occurrence of deep convection in the model. Current (e.g., Optical Transient Detector (OTD) and Lightning Imaging Sensor (LIS)) satellite measurements will eventually provide global climatologies of lightning flashes, but until that time climatologies, such as that by *Price et al.* [1997] derived from International Satellite Cloud Climatology Project (ISCCP) cloud data, will be relied upon for use in CTMs. Regardless of the source of the lightning geographic distribution, vertical distribution parameterizations will be necessary.

Some CTMs (e.g., IMAGES [*Müller and Brasseur*, 1995]) have assumed the lightning NO_x source to be uniform in terms of mass in the vertical. This assumption is counter to what is typically observed by aircraft in the outflow from convective storms, which is a maximum in the upper troposphere [e.g., *Dickerson et al.*, 1987; *Luke et al.*, 1992; *Ridley et al.*, 1996; *Pickering et al.*, 1996]. In the Geophysical Fluid Dynamics Laboratory (GFDL) CTM [*Levy et al.*, 1996] and in a regional CTM [*Flatøy and Hov*, 1997], lightning is produced in the parameterized subgrid convective clouds, and lightning NO_x is allowed to be redistributed by the vertical transport estimated in the convective parameterization scheme. The resulting vertical distribution of lightning NO_x is subject to the uncertainties associated with the convective parameterization which include location, frequency, and strength of convective cells. Neither *Levy et al.* [1996] or *Flatøy and Hov* [1997] present any resulting vertical distributions of NO_x from the lightning source.

In this paper we describe our method of specifying vertical distributions of lightning NO_x following redistribution by convective updrafts and downdrafts. We have taken the approach of using a detailed cloud-resolving model on a case study basis to simulate lightning flashes, NO production, and subsequent NO_x convective redistribution. To our knowledge, no two- or three-dimensional cloud model currently is capable of simulating both intracloud (IC) and cloud-to-ground (CG) lightning discharges from electrophysical principles and predicting the amount of NO_x produced per unit of energy released. We have therefore parameterized the lightning flash rate and placement using predicted dynamic and microphysical variables from the Goddard Cumulus Ensemble (GCE) model and use the model wind fields to redistribute the lightning NO_x. Upon dissipation of the simulated storm we integrate the lightning NO_x across the model domain in each layer and examine the resulting profile. Case study events were simulated in three environments (midlatitude continental, tropical continental, and tropical marine). The resulting vertical profiles can be used to specify the vertical distribution of the effective lightning NO_x source in regional and global CTMs. We demonstrate the effect on upper tropospheric NO_x and O_3 calculated in a global CTM resulting from changing from a uniform vertical distribution of the lightning NO_x source to use of the profiles developed here.

Section 2 of the paper describes our method of parameterization of lightning NO_x in the cloud model, and section 3 presents the results of seven case study events. We discuss the results and their implications in section 4.

2. Parameterization of Lightning NO_x Using Data From a Cloud-Resolving Model

We have developed a parameterization for lightning occurrence and NO_x production in association with the Goddard Cumulus Ensemble (GCE) model [*Tao and Simpson*, 1993]. The GCE model is a nonhydrostatic cloud-resolving model with detailed microphysics. The GCE model has been used for a number of chemical transport studies in observed deep convective events and has proven to accurately estimate vertical transport [e.g., *Pickering et al.*, 1996; *Stenchikov et al.*, 1996]. Model-computed fields of a number of variables are saved every 4 min throughout a cloud simulation and used as input for an off-line tracer transport model. We have placed our lightning NO_x scheme in the tracer transport model as described below.

The parameterization consists of four parts: flash rate, flash type, flash location, and NO production rate as described below. The flash parameterization is invoked in the tracer model every 4 min, and the advection scheme in the transport model performs transport calculations for NO_x (transported as ppbv NO_x with no chemistry) every 10 s.

2.1. Flash Rate

Although the exact mechanism of charge separation and lightning initiation remains incompletely understood, investigations of the relationship between lightning flash rate and various observed and simulated thunderstorm parameters are being conducted. For example, *Baker et al.* [1995] suggest through dimensional analysis and through a very simple 1-D model of microphysics and electrification that thunderstorm flash rate is roughly proportional to the sixth power of the vertical velocity. *Price and Rind* [1992] developed a parameterization for lightning flash rate that was used by *Price et al.* [1997] in developing a global lightning climatology based on ISCCP cloud data. The total flash rate (CG + IC flashes) in the Price and Rind work was estimated with empirical relationships using cloud-top height as the predictor. The relationships were derived from sets of field measurements relating flash rate to cloud height and cloud height with maximum vertical velocity. Lightning activity was also found to be positively correlated with updraft velocity. Intense updrafts tend to increase the depth of the charging zone leading to more efficient charge transfer between ice particles in the cloud resulting in more lightning. Flash rate data came from experiments involving northern hemisphere continental midlatitude thunderstorms [e.g., *Williams*, 1985]. These data also allow development of a relationship between flash rate and maximum vertical velocity in a thunderstorm given as equation (7) in the work of *Price and Rind* [1992]:

$$W = 14.66\, F^{0.22} \tag{1}$$

which can be rearranged to

$$F = 5 \times 10^{-6}\, W^{4.54} \tag{2}$$

where F is the flash rate (flashes per minute) for a convective cell and W is the maximum vertical velocity (m s^{-1}). The experimentally derived exponent of 4.54 is somewhat less than the value of ~6 derived theoretically by *Baker et al.* [1995].

We have decided to use the time evolution of maximum vertical velocity as computed from the GCE model to estimate flash rates throughout simulated storms using (2). There is some uncertainty in the use of this relationship for periods of

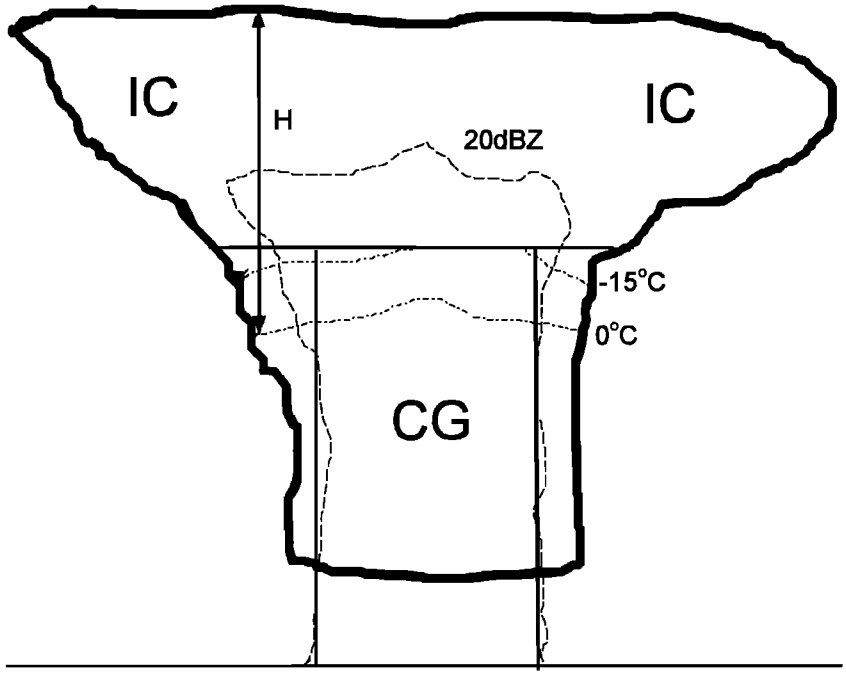

Figure 1. Schematic of lightning flash placement in the model. Heavy solid line represents cloud edge, dashed line is the 20 dbZ radar reflectivity contour, and dash-dotted lines are isotherms.

a few minutes throughout the evolution of a storm because the relationship (as well as the one between cloud-top height and flash rate) were developed using average flash rates, and maximum cloud-top heights and vertical velocities for storms. However, *Williams* [1985] indicates the relationships are valid for any timescale and presents time series data for cloud height and flash rate from a vigorous thunderstorm to support this argument. Similarly, *Weber et al.* [1993] present well-correlated time series of maximum vertical velocity and flash rate (data reproduced by *MacGorman and Rust* [1998]). In addition, the *Baker et al.* [1995] relationship was verified over the course of model simulations.

Price et al. [1997] applied the cloud height versus flash rate relationships to 5-km horizontal dimension instantaneous ISCCP pixels (representing individual cells) in developing a reasonable global lightning climatology. In our 2-D model we apply the vertical velocity versus flash rate relationship to the model-simulated width (front to rear) of the convective cell. For comparison of simulated flash rates to observations and for calculation of NO_x mixing ratios, we need to assume a dimension in the orthogonal horizontal direction. To be consistent with Price et al., we assume this dimension to be 5 km. However, *Williams* [1985] suggests a characteristic dimension similar to the cloud height (more typically 10–15 km).

2.2. Lightning Type

A scheme is needed to estimate the fraction of the total flash rate that is due to CG flashes versus that due to IC flashes. We have adapted the *Price and Rind* [1993] algorithm to estimate the fraction P of total flashes that are CG.

$$P = 1/(z + 1) \tag{3}$$

$$z = 0.021(\Delta H)^4 - 0.648(\Delta H)^3 + 7.493(\Delta H)^2 - 36.54(\Delta H) + 63.09 \tag{4}$$

where ΔH is the depth of the layer from the freezing level (the 0°C isotherm in the cloud) to the cloud top. We use the GCE model-generated temperature and hydrometeor fields in the calculation of ΔH. ΔH is computed after taking the average height of the 0°C isotherm across the model-generated cloud and the average height of where the computed total hydrometeor mixing ratio decreases to 10^{-5} g g^{-1} at the top of the cloud. The *Price and Rind* [1993] relationship was developed using cloud height and IC/CG ratio data for individual storms along with nearby radiosonde data. The parameterization is the best that exists and the only one that can be used in a model to differentiate between types of lightning. Uncertainty exists in the application of the relationship for periods of a few minutes throughout the evolution of a storm.

2.3. Flash Location

The placement of CG and IC flashes within the simulated cloud must also be considered. Simultaneous CG lightning flash and radar observations reported by *Rutledge and MacGorman* [1988] suggest that a very high percentage of the CG flashes occur within the regions of >20 dbZ radar reflectivity at low levels. Therefore we place the CG flashes within the region of the simulated storm having computed radar reflectivity >20 dbZ at 1 km altitude (see schematic in Figure 1). Radar reflectivity is computed in the GCE model using the size number distributions of precipitable hydrometeors (rain, snow, hail/graupel). CG flashes usually extend to the surface from the region of maximum negative charge in the cloud. *Houze* [1993] suggests the region in the cloud having temperature ~−15°C as being typically the region of maximum negative charge. Therefore we place the CG flashes within the 20 dbZ region from the surface to the model-calculated −15°C isotherm. *Ray et al.* [1987] and *Proctor* [1991] have shown that less energetic flashes (typically the IC flashes) tend to occur at higher altitude than the more energetic (mostly CG) flashes. Therefore we

Table 1. Convective Event Simulations

Event	CAPE*, $m^2 s^{-2}$	Horizontal Resolution, km	Reference
	Midlatitude Continental		
June 10–11, 1985, PRE-STORM	2300	1.0	*Pickering et al.* [1992] *Tao et al.* [1993]
June 26–27, 1985, PRE-STORM	2315	0.75	*Scala et al.* [1993]
	Tropical Marine		
Feb. 22, 1993, TOGA-COARE	1418	0.75	*Wang et al.* [1996]
Feb. 2–3, 1987, EMEX/STEP	1484	0.75	*Pickering et al.* [1993] *Tao et al.* [1993]
Sept. 12, 1974, GATE	1580	1.0	*Ferrier et al.* [1996]
	Tropical Continental		
Sept. 26–27, 1992, TRACE A	1100	1.0	*Pickering et al.* [1996]
April 26, 1987, ABLE 2B	2417	0.75	*Scala et al.* [1992]

*CAPE, convective available potential energy.

place the IC flashes in the region of the cloud above the −15°C isotherm. CG and IC flashes are assumed to distribute uniformly within their respective regions.

2.4. Lightning NO_x Production

Price et al. [1997] combined their estimates of energy per flash with a selected best estimate of NO production per unit energy from available literature to obtain NO production per flash values for CG and IC flashes. We have adopted the *Price et al.* [1997] values of 6.7×10^{26} molecules NO per CG flash and 6.7×10^{25} molecules NO per IC flash for use in our model. We have used these values because they were derived using a new formulation for the production of energy in lightning discharges and calculates the NO production based on the energy of the flash, which appears to be different in IC and CG flashes and different between positive and negative CG flashes. *Goldenbaum and Dickerson* [1993] suggest that NO production in lightning flashes is proportional to atmospheric pressure. In our model calculations we have assumed that the NO production during a flash is proportional to air density along the vertical extent of the flash because density is the variable used by the GCE model. The NO from the flashes estimated for each 4-min period is placed in the IC and CG regions of the simulated cloud in a bulk fashion, not along any particular channels. Therefore short-term local peaks of NO_x due to individual flashes do not appear in our model results.

3. Case Studies

We have run the cloud model lightning scheme for seven case study convective events representing three types of environments: (1) midlatitude continental; (2) tropical marine; and (3) tropical continental (see Table 1). Each of the convective events is taken from an intensive field project in which a variety of data (e.g., satellite, radar, soundings, aircraft, lightning, or air chemistry) are available for use in verifying the cloud model. In all seven cases the 2-D GCE model produced a simulated cloud reasonably similar to the observed, based on comparisons of model values and observations for variables such as cloud-top height, horizontal dimension, radar reflectivity, vertical velocity, precipitation, or tracer mixing ratios. Table 1 lists references for each case in which further details concerning the cloud simulation may be obtained. None of the field experiments were explicitly a lightning NO_x experiment; therefore not all of the desired types of data are available for each case. We have been unable to perform simulations for any midlatitude marine events because to our knowledge there have been no field programs of appropriate type conducted in this regime.

3.1. Midlatitude Continental Events

The first midlatitude event that we consider is the Kansas-Oklahoma squall line of June 10–11, 1985, during the Preliminary Regional Experiment for STORM (PRE-STORM) experiment. This was a very well-documented event which has been the subject of many observational [e.g., *Johnson and Hamilton*, 1988; *Rutledge et al.*, 1988] and modeling [e.g., *Zhang et al.*, 1989] papers in the literature. We have previously reported on the simulation of this storm with the GCE model [*Tao et al.*, 1993] and with tracer transport and photochemical models ([*Pickering et al.*, 1992], neglecting the influence of lightning). As reported in these references, the 2-D GCE model simulation of this event was verified against Doppler radar based wind and convective-stratiform structure, as well as satellite data.

Figure 2 shows the time series of model-calculated maximum vertical velocity and flash rates. Major flash rate and vertical velocity fluctuations on the timescale of 20–30 min reflect the lifetimes of individual convective cells. The lightning parameterization based on 2-D GCE model variables produced 81 CG flashes over the life cycle of the squall line. Observations of CG flashes from the lightning detection network in place during PRE-STORM compiled by *Rutledge and MacGorman* [1988] and *Nielsen et al.* [1994] show that after correction for ~70% detection efficiency there were an average of 22.5 CG flashes per kilometer along the squall line. Therefore, because we have assumed that the *Price and Rind* [1992] empirical relationship between flash rate and vertical velocity is appropriate for a horizontal dimension of 5 km along the squall line, we compare the observed number of flashes over a 5-km length of the squall line (113 flashes) with the model estimate. We find that the model-produced 81 CG flashes is approximately 75% of the observed CG flashes. Because there was a considerable amount of scatter in the data used by Price and Rind in developing flash rate relationships, we are justified in adjusting the value of the equation (2) exponent to produce a number of simulated flashes matching the number observed. An exponent of 4.76 was necessary in

this case to obtain 113 CG flashes. The time evolution of the CG and total flashes using this value is given in Figure 2.

NO_x from lightning is transported by the 2-D model-generated wind field throughout the simulation. Plate 1 shows the evolution of the NO_x field with time for the June 10–11 PRE-STORM event. Maxima develop in the anvil region of the storm and in the boundary layer to the rear of the storm. These maxima peak at approximately 5 ppbv at 4 hours into the simulation. Anvil (7–16 km) average NO_x was ~1.4 ppbv at this time. NO_x from IC flashes that were placed within the anvil, as well as that transported in updrafts from CG flashes at lower altitudes, contributed to the anvil maximum. A strong rear inflow at midlevels of the storm fed the downdrafts that descended and flowed near the surface toward the rear of the storm, bringing a portion of the CG NO_x downward and forming the second maxima in the boundary layer. Unfortunately, no NO_x measurements were made in the anvil or in the boundary layer near this storm. However, 5 days later in a storm with a roughly similar number of lightning flashes, *Dickerson et al.* [1987] measured 10-s average NO_x up to 6 ppbv and a 3-min average value of 4 ppbv in the anvil. On the basis of measurements in the boundary layer ahead of this later storm it appeared that approximately 1 ppbv was available for vertical transport. Therefore we believe that our anvil maximum of 5 ppbv NO_x is appropriate for the June 10–11 storm.

We converted the mixing ratios to mass units (g N) and integrated the mass across the model domain in each 1-km deep layer. Figure 3 shows the vertical distribution of N in lightning NO_x upon dissipation of the storm, expressed as percentages of the total produced in the storm. In the June 10–11 event we obtain maxima in the mass distribution in the upper tropospheric anvil region and in the lowest kilometer. Thus we obtain a vertical profile that is "C-shaped" between the surface and 12–13 km and then tapers to zero at 15–16 km. The tropopause was at approximately 14 km prior to this event. Therefore the model results suggest that there may have been a very small amount of lightning NO_x transported into the lower stratosphere by overshooting cloud tops. The "C-shaped" profile is similar to that suggested by *Lyons et al.* [1994] for lightning NO_x after convective redistribution.

The second midlatitude continental event was associated with a cold front crossing western Oklahoma on June 26, 1985, also during the PRE-STORM experiment. This event was documented by *Trier et al.* [1991], and GCE simulations for tracer transport without lightning were reported by *Scala et al.* [1993]. Vertical velocities in the simulated storm reached 20 to 25 m s^{-1}, but only for a period of about 20 min. For much of the simulation, maximum vertical velocities were in the 10–15 m s^{-1} range. Our estimated 5 CG flashes for this storm is much less than for the June 10–11 event. Thus our model indicates 1 CG flash per kilometer along the line of convection associated with this cold front. Lightning network data also show considerably fewer CG flashes (an average of only about 2 per kilometer along the line versus 22.5 flashes per kilometer for the June 10–11 case). We again adjusted the equation (2) exponent such that the simulation matched the observed number of CG flashes. In this case an exponent of 4.68 was required.

The NO_x tracer transport calculations for the June 26 case are shown in Figure 4. Maximum mixing ratios are reached after 4 hours of simulation, showing a peak of 1–1.5 ppbv in the rear anvil of the storm and a peak of 0.1–0.5 ppbv in the boundary layer behind the system. As expected, with the much

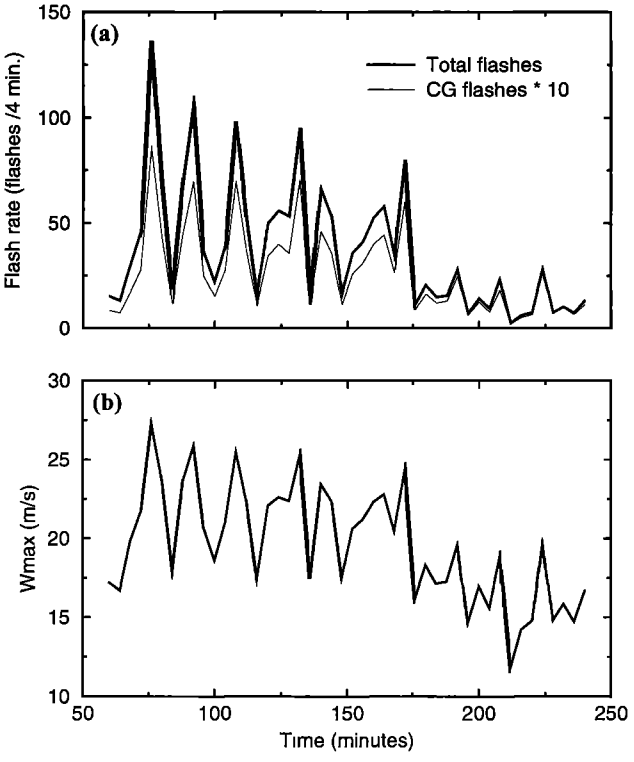

Figure 2. (a) Flash rate versus time; (b) maximum vertical velocity W versus time for June 10–11, 1985, PRE-STORM squall line simulation.

lower vertical velocities and flash rates, this storm produced much less NO_x than did the June 10–11 squall line. Upper tropospheric cloud outflow from this system was sampled by the National Center for Atmospheric Research (NCAR) Sabreliner [*Luke et al.*, 1992]. Sampling conducted at an altitude of 10 km at the forward edge of the anvil showed ~0.3 ppbv of NO_x. GCE model transport calculations for NO_x without lightning show that almost all of this NO_x in the forward anvil can be accounted for by transport from the boundary layer, suggesting that the effect of lightning on NO_x in this part of the storm was small. Indeed, our estimate in this portion of the anvil is less than 0.1 ppbv.

Figure 3 shows the vertical profile of percentage of total lightning NO_x mass (computed in g N) after integration across the model domain upon dissipation of the storm. In this case the anvil maximum is sharply peaked in the 12–13 km layer and therefore not as deep as in the June 10–11 squall line. Again, there is a pronounced maximum in the mass distribution in the 0–1 km layer, suggesting strong downdrafts. In this event a greater percentage of the mass is deposited in the 5–9 km midtropospheric layer than was computed for the June 10–11 event.

3.2. Tropical Marine Events

We consider three tropical marine events: (1) the February 22, 1993, squall line from the Tropical Ocean Global Atmosphere-Coupled Ocean Atmosphere Research Experiment (TOGA-COARE) project in the western Pacific; (2) the February 2–3, 1987, mesoscale convective complex from the Equatorial Mesoscale Experiment and Stratosphere-Troposphere Exchange Project (EMEX/STEP) in the region between Australia and New Guinea; and (3) the September 12, 1974, squall

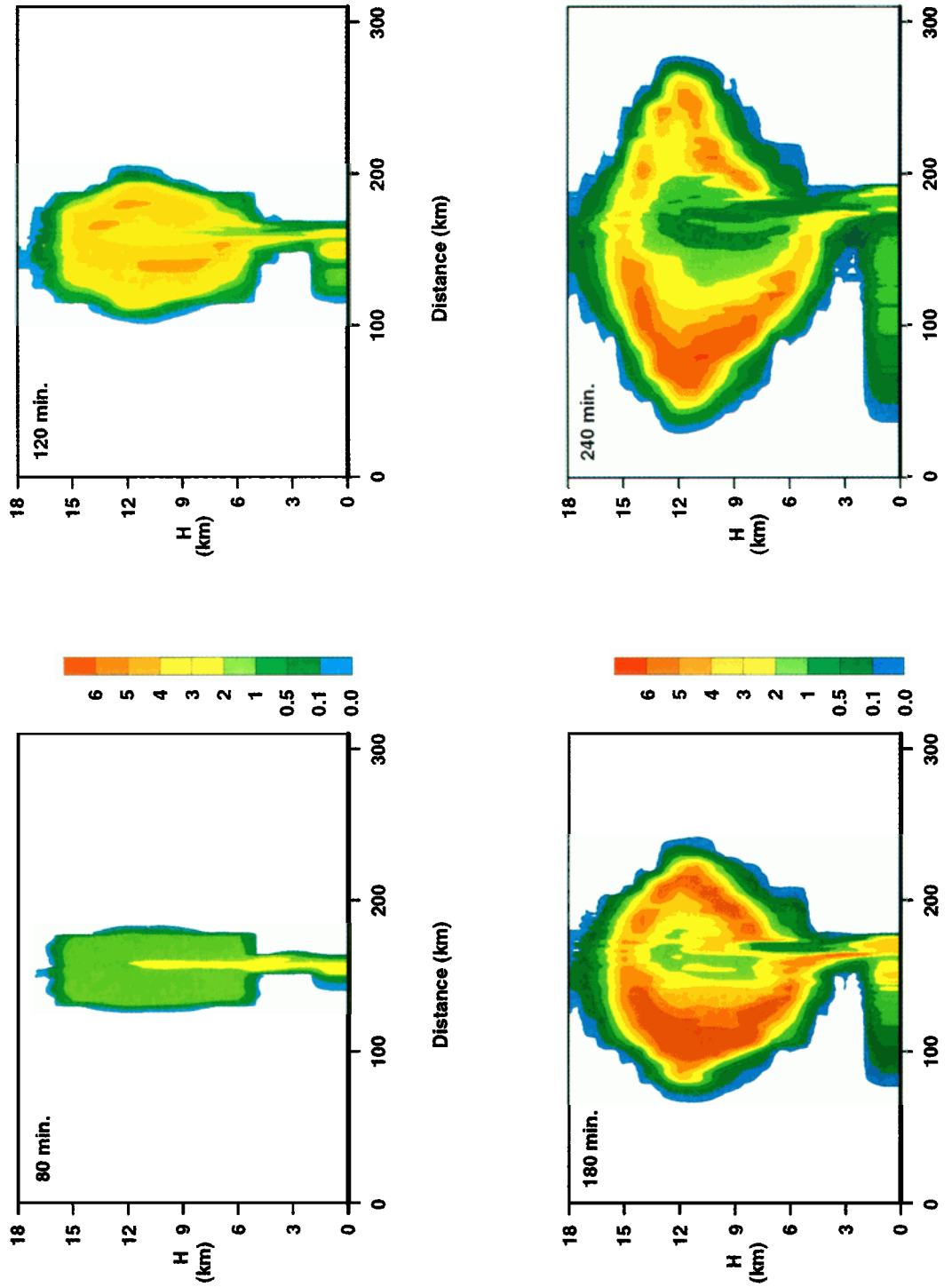

Plate 1. Lightning NO_x (ppbv) distributions for 80, 120, 180, and 240 min in the simulation of the June 10–11, 1985, PRE-STORM squall line.

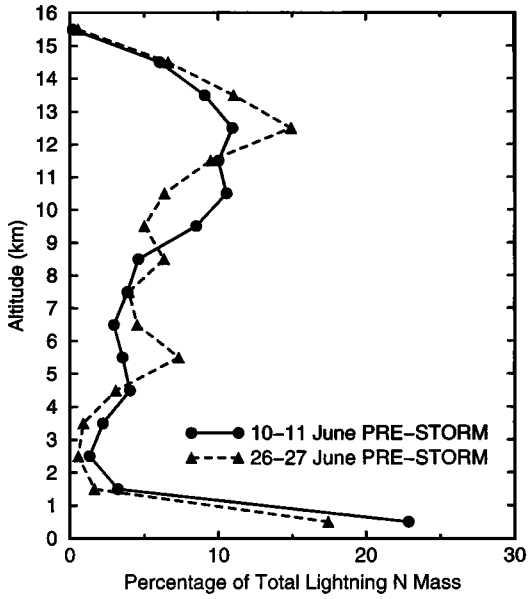

Figure 3. Vertical distributions of the percentage of total lightning NO_x mass (computed as mass of N) for two midlatitude continental simulations.

line from Global Atmospheric Research Project (GARP) Atlantic Tropical Experiment (GATE) over the Atlantic off West Africa. Unfortunately, the latter two events had no lightning detection system in place during the project. There was such a network during TOGA-COARE, but the squall line of interest was on the eastern edge of the coverage area. However, the NASA ER-2 aircraft performed overflights over this system providing electric field change data from which flash rates have been estimated.

The structure and evolution of the February 22 TOGA-COARE squall line near Guadalcanal in the Solomon Islands have been described by *Trier et al.* [1996], and GCE model simulations have been discussed by *Wang et al.* [1996]. The 2-D GCE model simulation produced maximum vertical velocities that were mostly in the 7–11 m s^{-1} range (somewhat smaller than in the Trier et al. 3-D simulation). The *Price and Rind* [1992] formulation (equation (2)) produces negligible lightning with these weak vertical velocities. However, ER-2 electric field change measurements taken over this storm show flash rates of 1–2 flashes per minute [*Orville et al.*, 1997]. Therefore

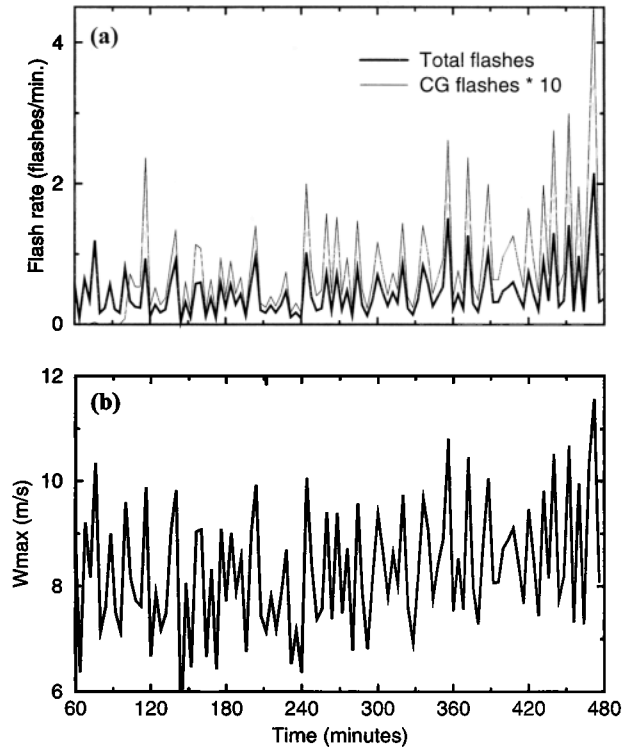

Figure 5. (a) Flash rate versus time; (b) maximum vertical velocity W versus time for February 22, 1993, TOGA-COARE squall line simulation.

we adjusted the exponent in (2) until our results matched the observed flash rate (see Figure 5). This required an increase of the exponent from 4.54 to 5.3.

NO_x mixing ratios show a dominant maximum in the upper tropospheric anvil region (Figure 6). The maximum values with the observed total flash rate reached 0.7–0.9 ppbv between 11 and 13 km by 7 hours into the simulation, and some smaller values reached to 16 km. These NO_x mixing ratios are roughly similar to those reported by *Chameides et al.* [1987] for anvil penetrations of two tropical convective cells over the Pacific. Figure 7 shows the vertical mass distribution after 7 hours of simulation. Only about 7.5% of the lightning-produced N mass is in the lowest kilometer because of the very weak downdrafts in this storm. In fact, the percentages are small up through the 6–7 km layer. About three fourths of the total lightning effect

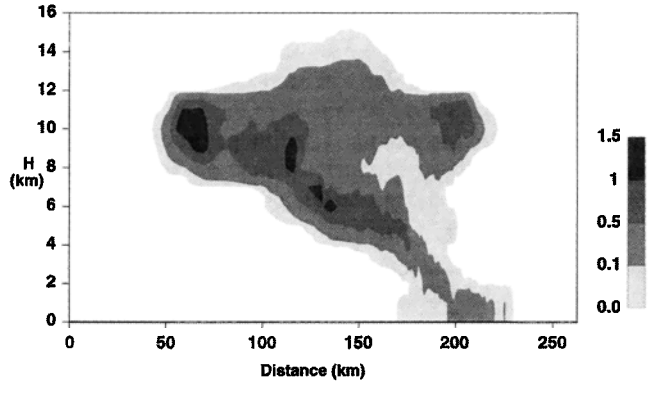

Figure 4. Lightning NO_x (ppbv) distribution for June 26–27, 1985, PRE-STORM simulation at time equal to 4 hours.

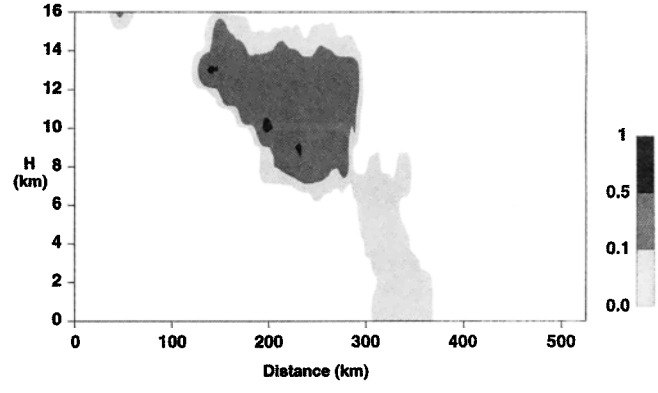

Figure 6. Lightning NO_x (ppbv) distribution for February 22, 1993, TOGA-COARE simulation at time equal to 7 hours.

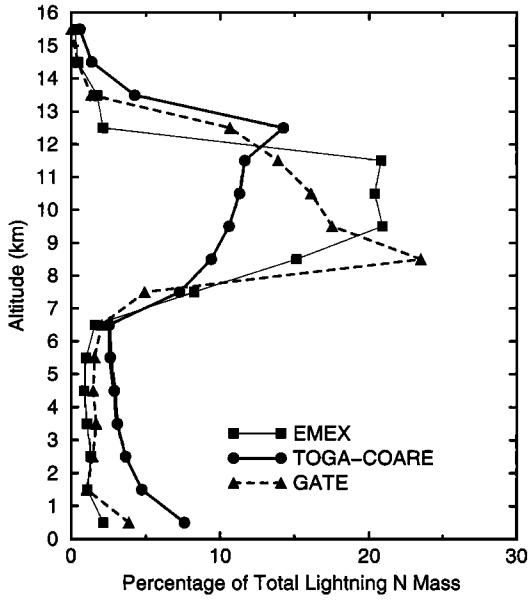

Figure 7. Vertical distributions of the percentage of total lightning NO_x mass (computed as mass of N) for three tropical marine cases.

on NO_x is above 7 km in this case, with the mass peaking in the 12–13 km layer.

The second tropical marine case was taken from GATE. In this long-lived convective event the simulated [*Ferrier et al.*, 1996] vertical velocities exceeded 10 m s^{-1} during a substantial portion of the simulated storm, reaching 15 m s^{-1} as a maximum (Figure 8). In this case we do not adjust the equation (2) exponent because we have no lightning data. With the exponent of 4.54 we obtain flash rates generally less than 0.5 min^{-1}, but reaching 0.75 min^{-1} and 1.5 min^{-1} in two more intense periods of the storm. At the 10-hour point in the simulation, NO_x remains <0.1 ppbv throughout a large region of the anvil (Figure 9). Flash rates and NO_x possibly may have been greater than what the model estimates with the 4.54 exponent because in all cases in which we have lightning data an increase of the exponent was necessary to match observations.

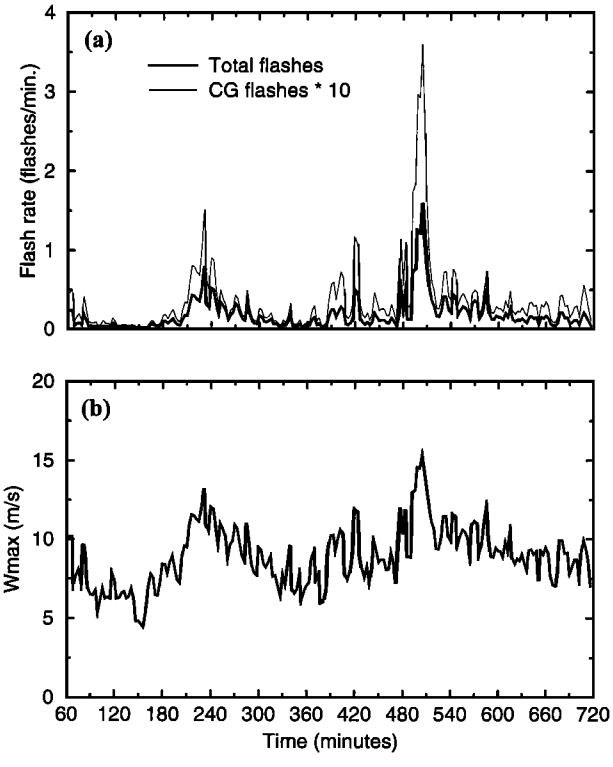

Figure 8. (a) Flash rate versus time; (b) maximum vertical velocity W versus time for September 12, 1974, GATE squall line simulation.

The vertical profile (Figure 7) for the GATE case is significantly different from that for the TOGA-COARE event. The upper tropospheric maximum (in percent) is at a lower altitude than in the TOGA-COARE event, and the percentage of the total lightning NO_x mass in the lowest kilometer is less than that in TOGA-COARE by approximately a factor of 2.

The third tropical marine case occurred over the Arafura Sea between Australia and New Guinea on February 2–3 1987, during the Equatorial Mesoscale Experiment (EMEX) and Stratosphere-Troposphere Exchange Project (STEP). With the exponent of 5.3 in the flash rate versus vertical velocity relationship we obtain no lightning flashes because vertical velocities were relatively small (they did not exceed 10 m s^{-1} at any time in the simulation, in agreement with NOAA P-3 aircraft observations). This result is in agreement with NO_y data taken by the NASA ER-2 aircraft in the upper part of the storm anvil [see *Pickering et al.*, 1993]. NO_y was depleted in this region as a result of upward transport of low NO_y air from the marine boundary layer. No enhancements of NO_y due to lightning were noted in the measurements near this storm.

As a hypothetical experiment to determine what the profile of lightning NO_x would have been like in the February 2–3, 1987, STEP/EMEX storm if there had been some lightning, we increased the exponent in the flash versus vertical velocity relationship until we obtained one CG flash in a 4-min time step. This required an exponent of 5.5. The resulting NO_x was almost entirely in the upper troposphere (see Figure 7) since downdrafts were extremely weak in this system.

3.3. Tropical Continental Events

We have considered two tropical continental events (1) the September 26–27, 1992, mesoscale convective system observed during the NASA Global Tropospheric Experiment (GTE) mission Transport and Atmospheric Chemistry Near the Equatorial Atlantic (TRACE A) over the cerrado region of Brazil;

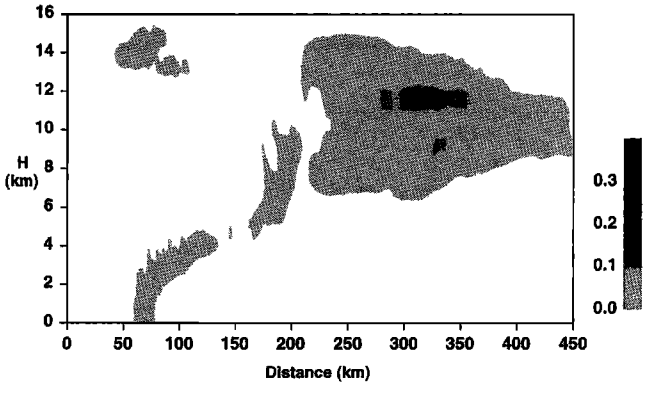

Figure 9. Lightning NO_x (ppbv) distribution for September 12, 1974, GATE simulation at time equal to 10 hours.

and (2) the April 26, 1987, squall line observed during the NASA GTE Amazon Boundary Layer Experiment (ABLE 2B) near Manaus, Brazil.

Unfortunately, there were no lightning flash data measured during the Brazilian phase of the TRACE A experiment. However, there were air chemistry measurements made from the NASA DC-8 aircraft early in the morning of September 27, 1992, in the outflow from two mesoscale convective systems that had been active overnight [*Pickering et al.*, 1996]. We have simulated a cell from the more southerly of these two systems with the GCE model. The portion of the DC-8 flight that passed through the outflow from this system was at 9.5 km, and the maximum 3-min average NO_x measurement during this flight segment was ~1.3 ppbv. Convective transport calculations reported by *Pickering et al.* [1996] show that the maximum amount of NO_x transported from the boundary layer to 9.5 km was about 0.4 ppbv. Therefore, at most, the contribution from lightning at this level would have been ~0.9 ppbv. A similar estimate of the lightning contribution based on the measured NO_x to CO ratios was obtained for this 3-min period [*Pickering et al.*, 1996]. In our lightning simulation of this event we found that with the exponent of 4.54 in the flash rate versus vertical velocity relationship our estimate of maximum lightning NO_x at 9.5 km was <0.1 ppbv. We found that an exponent of 5.13 was necessary to match the 0.9 ppbv of NO_x at 9.5 km (see Figure 10). Maximum vertical velocities in our simulation were between 10 and 20 m s^{-1} during the first 2 hours, but then remained less than 10 m s^{-1} for the remainder of the simulation. Therefore the bulk of the flashes were in these first 2 hours. The resulting vertical profile of lightning NO_x after redistribution by the TRACE A storm updrafts and downdrafts is shown in Figure 11. A very pronounced peak in this profile was formed in the upper troposphere (maximum percentage in the 13–14 km layer). A minimum in the profile appears between 4 and 6 km, with only slightly over 1% of the total lightning N mass in each of these two 1-km deep layers. Downdrafts were not particularly strong in the TRACE A system, but nearly 10% of the total lightning N mass exists in the lowermost kilometer upon dissipation of the storm.

GCE model simulations of the April 26, 1987, event from ABLE 2B have been documented by *Scala et al.* [1992], and chemical transport calculations have been reported by *Pickering et al.* [1992]. *Greco et al.* [1990] have shown that this squall line originated along the northern coast of South America and had moved southward into the vicinity of Manaus where the effects of the storm on trace gas distributions were studied with the NASA Electra aircraft. Unfortunately, no lightning detection measurements were made in ABLE 2B, and the aircraft was not capable of sampling upper tropospheric convective outflow.

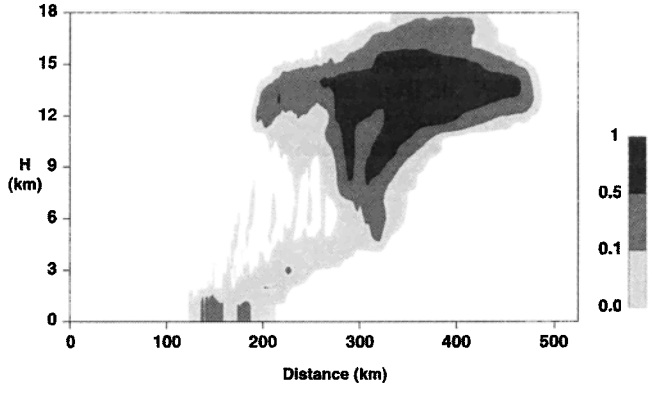

Figure 10. Lightning NO_x (ppbv) distribution for September 26–27, 1992, TRACE A convective system at time equal to 6 hours.

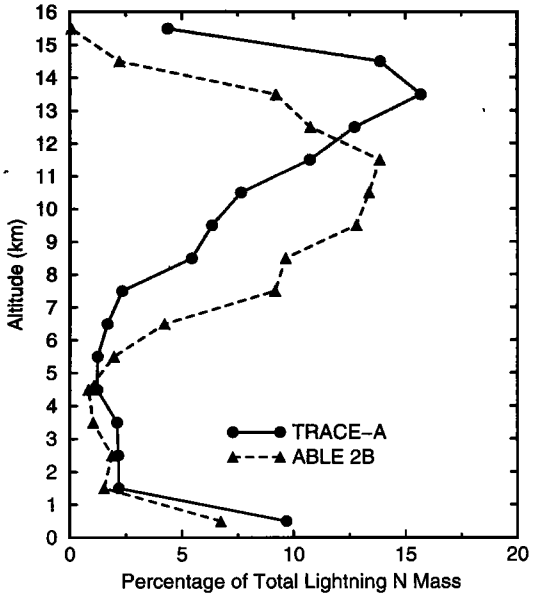

Figure 11. Vertical distributions of the percentage of total lightning NO_x mass (computed as mass of N) for two tropical continental cases.

The GCE model simulation produced very strong updrafts in this squall line reaching 25 m s^{-1} during two periods and remaining above 10 m s^{-1} continuously during the first 4.5 hours of the simulation. We use the value of 4.54 for the equation (2) exponent because we lack lightning and cloud outflow NO_x measurements for this event. These relatively high vertical velocities produced simulated lightning NO_x mixing ratios up to 1.5 ppbv within the anvil and updraft region and up to ~1 ppbv in the boundary layer (Figure 12). These values may be conservative given that exponents greater than 4.54 were required in the cases with observed lightning or NO_x. The profile of redistributed lightning NO_x for this event appears in Figure 11. The anvil maximum for the ABLE 2B case covers a broader altitude range than in the TRACE A event and peaks in the 11–12 km range. The minimum in the profile drops to ~1% in the 4–5 km layer, and the downdraft-induced maximum in the lowest kilometer reaches ~7%.

3.4. Average Profiles

Figure 13 presents profiles of lightning N mass distribution that have been computed by averaging profiles from the various cases in each of the three environments considered. Note that the profile from the EMEX/STEP event has been excluded from the average profile for the tropical marine regime because it resulted from a hypothetical model experiment. Table 2 lists the percentages for each 1-km layer, such that these values can readily be used by global and regional modelers. All three regions show an upper tropospheric maximum that results from a combination of upward transport of CG flash emissions in storm updrafts and production from IC flashes in the upper portion of the cloud. For the systems we

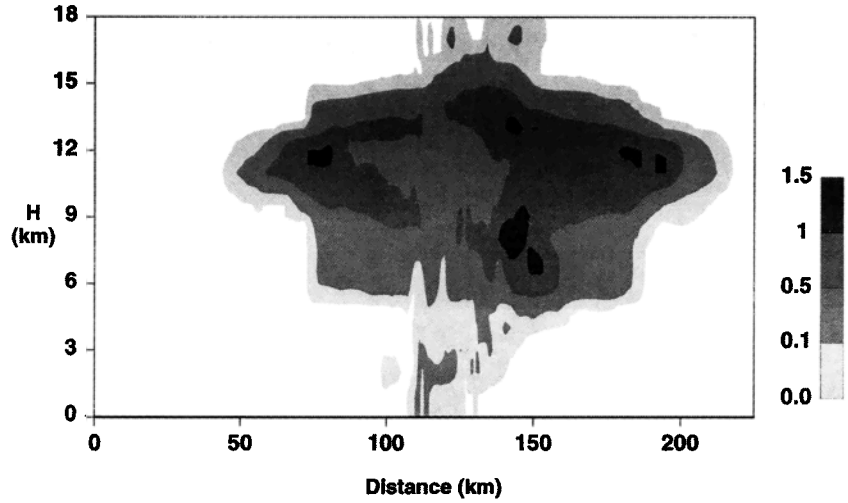

Figure 12. Lightning NO_x (ppbv) distribution for April 26, 1987, ABLE 2B simulation at time equal to 5 hours.

have simulated, the lightning NO_x profile extends to the highest altitude in the tropical continental environment (peak at 13–14 km), while the tropical marine systems tended to have their upper tropospheric maxima at the lowest altitude (8–12 km). Storms in all three environments produced minima in the profiles of 1–2% per 1-km layer. The minimum for continental midlatitude storms was less deep than in the tropical convection (i.e., a pronounced minimum in the 2–4 km layer). In the tropical systems the minimum extended from 1 to 7 km. Downdrafts were much stronger in the midlatitude systems, producing a maximum in the lowest kilometer of over 20% of the total lightning N mass. The percentage in the lowest kilometer for tropical continental systems was much lower (~8%) and even lower for tropical marine systems (~6%). Midlatitude convective systems more frequently can tap a source of cold, dry midtropospheric air to aid in downdraft formation.

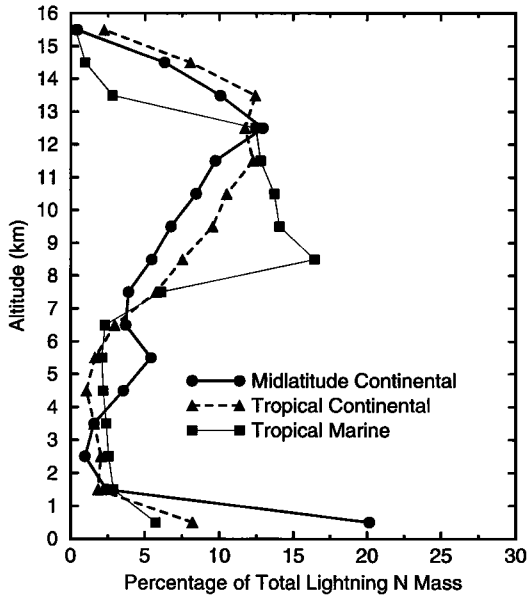

Figure 13. Average vertical distribution of percentage of lightning NO_x mass (computed as mass of N) for each of three regimes.

4. Discussion

4.1. Applications

A preliminary version of the profiles we derived in section 3 has been used to specify the vertical distribution of the lightning NO_x source in global chemical transport calculations presented by *Friedl* [1997] and *Penner et al.* [1998] and has been implemented in the Harvard CTM [*Y. Wang et al.*, 1998]. The preliminary version consisted of early results from one representative case from each of the three environments. The cases used were the June 10–11 PRE-STORM event for midlatitude continental regions, the September 26–27 TRACE A event for tropical continental environments, and the February 2–3 EMEX/STEP event for tropical marine regions. These preliminary profiles differ slightly from the profiles for these events that appear in Figures 3, 7, and 11 due to 2 factors: (1) a

Table 2. Average Profiles of Lightning NO_x (N) Mass in Percent

Altitude Range, km	Midlatitude Continental	Tropical Marine	Tropical Continental
0–1	20.1	5.8	8.2
1–2	2.3	2.9	1.9
2–3	0.8	2.6	2.1
3–4	1.5	2.4	1.6
4–5	3.4	2.2	1.1
5–6	5.3	2.1	1.6
6–7	3.6	2.3	3.0
7–8	3.8	6.1	5.8
8–9	5.4	16.5	7.6
9–10	6.6	14.1	9.6
10–11	8.3	13.7	10.5
11–12	9.6	12.8	12.3
12–13	12.8	12.5	11.8
13–14	10.0	2.8	12.5
14–15	6.2	0.9	8.1
15–16	0.3	0.3	2.3

change in the cloud model simulation times selected as being representative of the end of convective transport in the events; and (2) a change in the exponent of the flash rate versus vertical velocity relationship used in the TRACE A event to more closely match observed NO_x values. Very little difference exists between the preliminary profile for the June 10–11 PRE-STORM event, the profile in Figure 3, and the average profile for midlatitude continental cases in Figure 13. The main difference for the tropical marine and tropical continental environments is that the final profiles for the EMEX/STEP and TRACE A cases, as well as the average profiles, are slightly more "C-shaped" than the preliminary ones. That is, there is more lightning NO_x mass (by a few percent) in the lowest kilometer in the final results for these cases, as well as in the average profiles for these regimes, than there was in the preliminary results.

In the work summarized by *Friedl* [1997] and that presented by *Penner et al.* [1998] the preliminary profiles were applied with the lightning NO_x climatology of *Price et al.* [1997] which is based on the deep convective cloud distribution from ISCCP. The tropical marine profile was applied for midlatitude marine convection. However, it is possible that in intense convection over midlatitude warm ocean currents (e.g., Gulf Stream) the potential for strong downdrafts may be present, making the midlatitude continental profile more appropriate. Our profiles were scaled to the heights of convective clouds as determined by ISCCP. In doing this scaling a comparison must be made between the ISCCP cloud-top altitude and the height of the tropopause in the model, so that large quantities of lightning NO_x are not injected into the stratosphere. However, in reality a small amount of lightning NO_x may sometimes enter the stratosphere during deep convection through overshooting cloud tops [e.g., *Poulida et al.*, 1996]. Alternatively, the lightning NO_x emissions can be placed in a model at the locations where deep convection is diagnosed by the convective parameterization, and our profiles can be used by scaling to the model-estimated cloud-top height, as is now done in the Harvard CTM [*Y. Wang et al.*, 1998].

Friedl [1997] reports results of NO_y tracer calculations performed with five different models all using the *Price et al.* [1997] lightning NO_x climatology and our preliminary profiles. Sources in addition to lightning were aircraft, the stratosphere, and surface sources (soils, fossil fuels, and biomass burning). All of the models demonstrated that most of the NO_y in the upper troposphere at northern midlatitudes in the summer is from surface sources and lightning. For example, in a CTM driven with NCAR Community Climate Model, Version 2 (CCM2) data, the lightning source is the largest contributor to NO_y in the midlatitude upper troposphere in July.

4.2. Implications for Ozone Production

The vertical profiles that we have computed in section 3 show that a large portion of the lightning NO_x ends up in the upper troposphere (within 2–4 km of the tropopause) following a thunderstorm. At these altitudes, NO_x has a much longer lifetime than in the boundary layer (several days versus ~1 day). NO_x is oxidized to nitric acid, but may be recycled back to NO_x in the upper troposphere [e.g., *Jacob et al.*, 1996]. Therefore the lightning NO_x has the potential to catalyze the production of substantial amounts of ozone in the upper troposphere. In section 4.2.1 we discuss our ozone production calculations in the outflow of specific storms. In section 4.2.2 we demonstrate that larger quantities of ozone will be produced in the upper troposphere of regional and global CTMs using these vertical distributions of the lightning NO_x source than would be obtained with the assumption of a uniform vertical distribution. This result has important implications because ozone at these altitudes is particularly effective as a greenhouse gas [e.g., *Lacis et al.*, 1990].

4.2.1. Ozone production for individual cases. *Pickering et al.* [1990] examined air chemistry data taken during the Oklahoma-Kansas PRE-STORM experiment [e.g., *Dickerson et al.*, 1987; *Luke et al.*, 1992] to identify periods in the data representative of outflow from specific convective systems. These measurements were then used to constrain a 1-D photochemical model in calculating rates of ozone production. In the event reported by *Dickerson et al.* [1987] it was estimated that at least three fourths of the up to 4 ppbv of NO_x found in the anvil was due to lightning based on the amount of NO_x available in the boundary layer for upward convective transport. *Pickering et al.* [1990] computed net ozone production rates of 5 ppbv d^{-1} at 11 km and 16 ppbv d^{-1} at 8 km in the cloud-processed air for the first 24 hours following this convective event. These values are factors of 2.5 and 3, respectively, greater than net ozone production rates in nearby air undisturbed by the storm.

Ozone production in outflow from mesoscale convective systems in Brazil during the biomass burning season was discussed by *Pickering et al.* [1996]. In the maximum outflow (highest 9-min or ~120-km average values) where NO_x was ~950 pptv a few hours after the storm, ozone production totaled 27.5 ppbv over the first 4 days of downwind transport. On the basis of the NO_x/CO ratio, at least 50% of the measured NO_x during this 9-min period was due to lightning. Transport of enhanced upper tropospheric NO_x (400–600 pptv) from lightning over central Brazil has also been detected along the Atlantic coast of Brazil by *Dickerson* [1984]. Lightning NO_x produced over South America makes a substantial contribution to the tropospheric ozone maximum observed over the South Atlantic [*Pickering et al.*, 1996].

Measurements taken onboard the NASA ER-2 in the vicinity of the STEP/EMEX storm of February 2–3, 1987 [*Pickering et al.*, 1993], showed no NO_y enhancements, consistent with our initial simulation producing no lightning flashes. Other portions of this flight showed strong lightning NO_y signals based on the NO_y/O_3 ratio, a technique first used in the upper troposphere by *Murphy et al.* [1993]. Air arriving at this portion of the flight appeared to contain outflow from upstream convection over coastal regions of northern Australia and perhaps other storms farther upstream. Between 12 and 16 km, *Pickering et al.* [1993] estimated that an average of 64% of the NO_x computed in the 1-D photochemical model (constrained with ambient NO_y, O_3, and CO measurements) was due to lightning. Calculations with the photochemical model to estimate ozone production rates over a 24-hour period showed that a factor of 2–3 more ozone was produced in this layer when the lightning NO_x was included than when it was not.

4.2.2. NO_x and O_3 in a global model. In order to demonstrate the relevance of the lightning NO_x profiles for global tropospheric chemistry, a sensitivity calculation has been performed using a global 3-D tropospheric CTM, the IMAGES model. This model has been described, and its results have been compared with a wide range of observations [*Müller and Brasseur*, 1995; *Friedl*, 1997; *Müller and Brasseur*, 1998]. Important model updates are described by *Müller and Brasseur* [1998], including acetone photochemistry and a revised de-

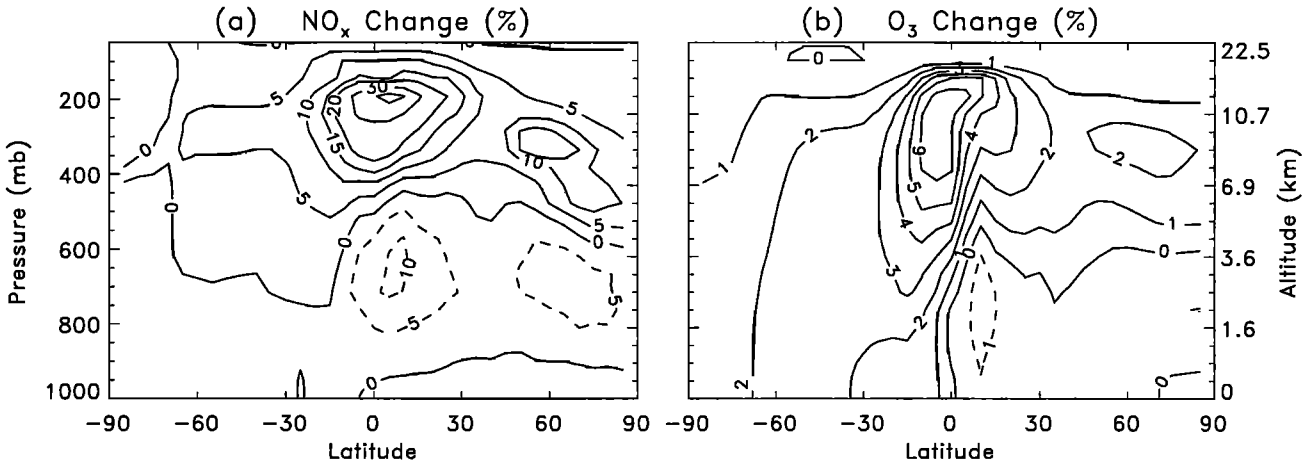

Figure 14. Calculated impact of the change from uniform to C-shaped vertical profiles of lightning emissions on zonally averaged mixing ratios of (a) NO_x and (b) O_3. The results are given in percent for July conditions. Negative isolines are dashed.

scription of convective scavenging of soluble gases. The lightning source is geographically distributed following *Price et al.* [1997] and is scaled to a global source of 3 Tg N yr^{-1} in the simulations described here.

Two runs of the model were performed: (1) with the uniform source profile of lightning NO_x; and (2) with the C-shaped profiles given in Table 2. The calculated impact of using the C-shaped profiles on zonally averaged NO_x and O_3 mixing ratios is displayed in Figure 14. The changes in the PBL are negligible. This was to be expected since the surface sources of NO_x are dominant near the surface over continents regardless of what profile is used for lightning NO_x. In the lower troposphere above the PBL (1–5 km) we note a slight decrease in NO_x (up to about −10%) and ozone (−1%). In the upper troposphere, however, NO_x mixing ratios are calculated to increase by up to 15–20% at midlatitudes and 45% at the equator. The change in ozone production (not shown) follows closely the change in NO_x, although with somewhat lower values, because of a significant decrease in HO_2 levels around the tropopause (up to ~10%). The changes in OH and HNO_3 levels also follow the changes in NO_x. The higher NO_x abundances result in an increase in upper tropospheric ozone, reaching about 7% near the equator. In the regions of most intense convection, NO_x mixing ratios as well as ozone production rates change by up to 60% at 10–14 km near the equator. These values would of course be higher when using a higher global lightning source.

4.3. Uncertainties

Uncertainties in our lightning NO_x profiles stem from a variety of sources: the case study events themselves, the GCE model simulations, and the parameterization of lightning and NO_x production. The convective events that we have simulated are representative of well-organized, relatively long-lived mesoscale convective systems (MCSs). These are events for which cloud-resolving models (including the GCE model) generally perform well. A variety of MCSs are represented: a midlatitude squall line, a convective line associated with a cold front, a tropical marine squall line, a nearly stationary tropical mesoscale convective cluster, and a large Amazon coastal occurring system. Other types of convective events (e.g., air mass thunderstorms, mesoscale convective complexes, supercells, etc.) are not as well-simulated with cloud models. We suspect that the types of convection not simulated here would produce roughly similar types of profiles as the ones we have calculated. We do know, however, that it is very likely that the assumption of uniform vertical lightning NO_x mass distribution that has been made in some CTMs is incorrect.

Uncertainties exist in all phases of our parameterization of lightning and NO_x production in the GCE model. The total flash rate is a very sensitive function of the model-calculated maximum vertical velocity (approximately fifth power). Therefore small errors in the estimate of vertical velocity will lead to substantial errors in lightning flash rate. For example, the updrafts computed in a 2-D cloud-resolving model tend to be somewhat weaker than those in 3-D simulations. However, we believe that in the examples shown in section 3 reasonable results using this method have been demonstrated for cases in which either flash rate or NO_x data were available. Uncertainty concerning flash placement mainly centers on whether a substantial fraction of the CG lightning occurs in downdraft regions. Our results for midlatitude continental storms show up to ~23% of the lightning NO_x mass existing in the lowest kilometer following convective transport. Aircraft observations to date have not been able to verify this type of result [e.g., *Ridley et al.*, 1996]. However, the results of *Ray et al.* [1987] showing simultaneous Doppler radar vertical velocities and lightning locations suggest that a significant amount of flashes occur in downdraft regions of some midlatitude storms.

We have tested the sensitivity of our results to our assumption of >20 dbZ radar reflectivity as the region within which CG flashes occur. We ran our algorithm in a sensitivity study for the June 10–11, 1985, PRE-STORM event, using criteria of 10, 15, 20, and 25 dbZ. The results showed negligible differences in the resulting lightning NO_x mass distribution profiles for this case.

Price et al. [1997] report approximately factor of 2 uncertainty in both the energy per flash and the number of NO molecules produced per unit of energy. Therefore uncertainties of these magnitudes will be reflected in our lightning NO_x mixing ratio results due to these production uncertainties. If actual NO production is greater or smaller than the values

assumed here, presumably the mixing ratios would be scaled up or down accordingly, and the shapes of the vertical profiles of lightning NO_x mass distributions would remain the same. Using their NO per flash values, *Price et al.* [1997] derived a global lightning NO_x production rate of 12.2 Tg N yr^{-1}, which is near the high end of the current commonly accepted range. However, using these same production per flash values along with numbers of flashes matching observed rates, we obtain values of NO_x mixing ratios in storms that are reasonable compared with observed NO_x observations. Greater uncertainty likely exists in the absolute values of the NO_x mixing ratios for the individual storms than in the shapes of the vertical profiles of postconvective lightning NO_x mass distribution. The assumption of IC flashes being 10% as energetic as CG flashes does have an influence on the resulting profiles. If, for example, IC flashes contained less than this amount of energy, the upper tropospheric peak in the mass profiles might not be as pronounced.

We have run lightning NO_x as a conserved tracer in these calculations over a period of a few hours. In reality, some fraction of the NO_x is oxidized to other reactive nitrogen compounds. However, in the lower portion of an convective storm we would expect that UV fluxes would be quite small due to the optically thick cloud, making oxidation reactions proceed very slowly. We have demonstrated that a large fraction of the lightning NO_x resides in the upper troposphere by the end of the storm. NO_x has a several day lifetime at these altitudes, making the conserved tracer assumption for a several hour period a close approximation.

5. Summary

We have developed a parameterization for lightning occurrence, type, placement, and NO_x production in a cloud-resolving model using model-calculated variables. Wind fields from the model are used to redistribute the lightning NO_x throughout the duration of a simulated storm. Seven convective events from three different regimes have been simulated using the lightning algorithm. Profiles of lightning NO_x mass distribution at the end of each storm have been computed and averaged over the storms in each regime. The results for all three regimes show a maximum in the mass profile in the upper troposphere. Downdrafts appear to be the strongest in the simulated midlatitude continental systems, evidenced by the substantial lightning NO_x mass (up to ~23%) in the lowest kilometer at the end of the storm. Tropical systems, particularly those over marine regions, tended to have a greater fraction of IC flashes and weaker downdrafts, creating the conditions for only minor amounts of NO_x remaining in the boundary layer at the end of a storm. Reasonable model estimates of lightning NO_x mixing ratios in storms have been obtained, but these are more uncertain than the vertical distribution profiles. The average profiles for the three regimes can be used to specify the vertical distribution of the lightning NO_x source in regional and global chemical transport models. We can conclude that the uniform lightning NO_x mass distribution used in some CTMs is incorrect. Changing to use of our vertical distributions produces increases in the amount of zonally averaged upper tropospheric NO_x and O_3 of up to 45 and 7%, respectively.

Field experiments with extensive radar, lightning, and chemistry observations are needed to further verify and improve our algorithm and reduce uncertainties. One such experiment, Stratosphere-Troposphere Experiments: Radiation, Aerosols, and Ozone (STERAO A) Deep Convection, was conducted in northeast Colorado in summer 1996. Data analysis and modeling are currently ongoing. We anticipate that improvements in our parameterization and the lightning NO_x profiles will result from this experiment. For example, the STERAO A data will help determine the validity of the flash rate versus maximum vertical velocity relationship and the IC/CG ratio formulation. It is also possible that separate criteria for CG flash placement in the convective and stratiform regions of a storm may be appropriate. Information concerning the 3-D placement of flashes within a storm may be provided from instrumentation deployed during the experiment. Recent laboratory experiments [*Y.-J. Wang et al.*, 1998] suggest that NO production may be better correlated with peak current in a flash than with energy per flash. We will investigate use of an NO production formulation using peak current in future simulations. In addition, a more electrophysically based scheme for lightning in the GCE model will be developed in the future.

Acknowledgments. This work was supported under NASA's Atmospheric Effects of Aviation Project. Development and improvement of the GCE model has been supported under the NASA Physical Climate Program. IMAGES calculations were supported by the Belgian Office for Scientific, Technological, and Cultural Affairs. We thank J. Scala (SUNY-Brockport) for access to cloud model output for two of the case studies, and R. Dickerson (University of Maryland) and D. Jacob (Harvard University) for helpful comments.

References

Baker, M. B., H. J. Christian, and J. Latham, A computational study of the relationships linking lightning frequency and other thundercloud parameters, *Q. J. R. Meteorol. Soc.*, *121*, 1525–1548, 1995.

Baughcum, S. L., T. G. Tritz, S. C. Henderson, and D. C. Pickett, Scheduled civil aircraft emission inventories for 1992, *NASA Contract. Rep.*, *CR-4700*, 1996.

Benkovitz, C. M., M. T. Sholtz, J. Pacyna, L. Tarrason, J. Dignon, E. C. Voldner, P. A. Spiro, J. A. Logan, and T. E. Graedel, Global gridded inventories of anthropogenic emissions of sulfur and nitrogen, *J. Geophys. Res.*, *101*, 29,239–29,253, 1996.

Chameides, W. L., D. D. Davis, J. Bradshaw, M. Rodgers, S. Sandholm, and D. B. Bai, An estimate of the NO_x production rate in electrified clouds based on NO observations from the GTE/CITE 1 fall 1983 field operation, *J. Geophys. Res.*, *92*, 2153–2156, 1987.

Dickerson, R. R., Measurements of reactive nitrogen compounds in the free troposphere, *Atmos. Environ.*, *18*, 2585–2593, 1984.

Dickerson, R. R., et al., Thunderstorms: An important mechanism in the transport of pollutants, *Science*, *235*, 460–465, 1987.

Ferrier, B. S., J. Simpson, and W.-K. Tao, Factors responsible for precipitation efficiencies in midlatitude and tropical squall simulations, *Mon. Weather Rev.*, *124*, 2100–2125, 1996.

Flatøy, F., and Ø. Hov, NO_x from lightning and the calculated chemical composition of the free troposphere, *J. Geophys. Res.*, *102*, 21,373–21,381, 1997.

Friedl, R. R., Atmospheric effects of subsonic aircraft: Interim assessment report of the Advanced Subsonic Technology Program, *NASA Ref. Publ.*, *1400*, 1997.

Goldenbaum, G. C., and R. R. Dickerson, Nitric oxide production by lightning discharges, *J. Geophys. Res.*, *98*, 18,333–18,338, 1993.

Greco, S., R. Swap, M. Garstang, S. Ulanski, M. Shipham, R. C. Harriss, R. Talbot, M. O. Andreae, and P. Artaxo, Rainfall and surface kinematic conditions over central Amazonia during ABLE 2B, *J. Geophys. Res.*, *95*, 17,001–17,014, 1990.

Houze, R. A., Jr., *Cloud Dynamics*, 573 pp., Academic, San Diego, Calif., 1993.

Jacob, D. J., et al., Origin of ozone and NO_x in the tropical troposphere: A photochemical analysis of aircraft observations over the South Atlantic basin, *J. Geophys. Res.*, *101*, 24,235–24,250, 1996.

Johnson, R. H., and P. J. Hamilton, The relationship of surface pres-

sure features to the precipitation and airflow structure of an intense midlatitude squall line, *Mon. Weather Rev.*, *116*, 1444–1472, 1988.

Lacis, A. A., D. J. Wuebbles, and J. A. Logan, Radiative forcing of climate by changes in the vertical distribution of ozone, *J. Geophys. Res.*, *95*, 9971–9981, 1990.

Lamarque, J.-F., G. P. Brasseur, P. G. Hess, and J.-F. Mueller, Three-dimensional study of the relative contributions of the different nitrogen sources in the troposphere, *J. Geophys. Res.*, *101*, 22,955–22,968, 1996.

Levy, H., II, W. J. Moxim, and P. S. Kasibhatla, A global three-dimensional time-dependent lightning source of tropospheric NO_x, *J. Geophys. Res.*, *101*, 22,911–22,922, 1996.

Luke, W. T., R. R. Dickerson, W. F. Ryan, K. E. Pickering, and L. J. Nunnermacker, Tropospheric chemistry over the lower Great Plains of the United States, 2, Trace gas profiles and distributions, *J. Geophys. Res.*, *97*, 20,647–20,670, 1992.

Lyons, W. A., J. L. Eastman, R. A. Peilke, A. Biazar, and R. McNider, A preliminary climatology of lightning-generated NO_x and numerical simulations of its redistribution by deep convection, paper presented at Conference on Atmospheric Chemistry, Am. Meteorol. Soc., Boston, Mass., 1994.

MacGorman, D. R., and W. D. Rust, *The Electrical Nature of Storms*, 422 pp., Oxford Univ. Press, New York, 1998.

Muller, J.-F., and G. P. Brasseur, IMAGES: A three-dimensional chemical transport model of the global troposphere, *J. Geophys. Res.*, *100*, 16,445–16,490, 1995.

Müller, J.-F., and G. P. Brasseur, Sources of upper tropospheric HO_x: A three-dimensional study, *J. Geophys. Res.*, in press, 1998.

Murphy, D. M., D. W. Fahey, M. H. Proffitt, S. C. Liu, K. R. Chan, C. S. Eubank, S. R. Kawa, and K. K. Kelly, Reactive nitrogen and its correlation with ozone in the lower stratosphere and upper troposphere, *J. Geophys. Res.*, *98*, 8751–8773, 1993.

Nielsen, K. E., R. A. Maddox, and S. V. Vasiloff, The evolution of cloud-to-ground lightning within a portion of the 10–11 June 1985 squall line, *Mon. Weather Rev.*, *122*, 1809–1817, 1994.

Orville, R. E., et al., Lightning in the region of the TOGA COARE, *Bull. Am. Meteorol. Soc.*, *78*, 1055–1067, 1997.

Penner, J. E., D. J. Bergmann, J. J. Walton, D. Kinnison, M. J. Prather, D. Rotman, C. Price, K. E. Pickering, and S. L. Baughcum, An evaluation of upper tropospheric NO_x with two models, *J. Geophys. Res.*, *103*, 22,097–22,113, 1998.

Pickering, K. E., A. M. Thompson, R. R. Dickerson, W. T. Luke, and D. P. McNamara, Model calculations of tropospheric ozone production potential following observed convective events, *J. Geophys. Res.*, *95*, 14,049–14,062, 1990.

Pickering, K. E., A. M. Thompson, J. Scala, W.-K. Tao, R. R. Dickerson, and J. Simpson, Free tropospheric ozone production following entrainment of urban plumes into deep convection, *J. Geophys. Res.*, *97*, 17,985–18,000, 1992.

Pickering, K. E., A. M. Thompson, W.-K. Tao, and T. L. Kucsera, Upper tropospheric ozone production following mesoscale convection during STEP/EMEX, *J. Geophys. Res.*, *98*, 8737–8749, 1993.

Pickering, K. E., et al., Convective transport of biomass burning emissions over Brazil during TRACE A, *J. Geophys. Res.*, *101*, 23,993–24,012, 1996.

Poulida, O., R. R. Dickerson, and A. Heymsfield, Stratosphere-troposphere exchange in a midlatitude mesoscale convective complex, 1, Observations, *J. Geophys. Res.*, *101*, 6837–6852, 1996.

Price, C., and D. Rind, A simple lightning parameterization for calculating global lightning distributions, *J. Geophys. Res.*, *97*, 9919–9933, 1992.

Price, C., and D. Rind, What determines the cloud-to-ground fraction in thunderstorms?, *Geophys. Res. Lett.*, *20*, 463–466, 1993.

Price, C., J. Penner, and M. Prather, NO_x from lightning, 1, Global distribution based on lightning physics, *J. Geophys. Res.*, *102*, 5929–5941, 1997.

Proctor, D. E., Regions where lightning flashes began, *J. Geophys. Res.*, *96*, 5099–5112, 1991.

Ray, P. S., D. R. MacGorman, W. D. Rust, W. L. Taylor, and L. R. Rasmussen, Lightning location relative to storm structure in a supercell and a multicell storm, *J. Geophys. Res.*, *92*, 5713–5724, 1987.

Ridley, B. A., J. E. Dye, J. G. Walega, J. Zheng, F. E. Grahek, and W. Rison, On the production of active nitrogen by thunderstorms over New Mexico, *J. Geophys. Res.*, *101*, 20,985–21,005, 1996.

Rutledge, S. A., and D. R. MacGorman, Cloud-to-ground lightning activity in the 10–11 June 1985 convective system observed during the Oklahoma-Kansas PRE-STORM project, *Mon. Weather Rev.*, *116*, 1393–1408, 1988.

Rutledge, S. A., R. A. Houze Jr., M. I. Biggerstaff, and T. Matejka, The Oklahoma-Kansas mesoscale convective system of 10–11 June 1985: Precipitation structure and single-Doppler radar analysis, *Mon. Weather Rev.*, *116*, 1409–1430, 1988.

Scala, J. R., W.-K. Tao, and J. Simpson, Transport dynamics in the convective and stratiform regions of a tropical squall line: Results of a two-dimensional numerical investigation, paper presented at Fifth Conference on Mesoscale Processes, Am. Meteorol. Soc., Atlanta, Ga., 1992.

Scala, J. R., K. E. Pickering, W.-K. Tao, J. Simpson, and R. R. Dickerson, Convective transport and mixing of tracers by midlatitude squall-type mesoscale convective systems, paper presented at Conference on Atmospheric Chemistry, Am. Meteorol. Soc., Anaheim, Calif., 1993.

Stenchikov, G., R. Dickerson, K. Pickering, W. Ellis. B. Doddridge, S. Kondragunta, O. Poulida, J. Scala, and W.-K. Tao, Stratosphere-troposphere exchange in a midlatitude mesoscale convective complex, 2, Numerical simulations, *J. Geophys. Res.*, *101*, 6837–6851, 1996.

Tao, W.-K., and J. Simpson, The Goddard Cumulus Ensemble Model, I, Model description, *Terr. Atmos. Oceanic Sci.*, *4*, 35–72, 1993.

Tao, W.-K., J. Simpson, C.-H. Sui, B. Ferrier, S. Lang, J. Scala, M.-D. Chou, and K. Pickering, Heating, moisture, and water budgets of tropical and midlatitude squall lines: Comparisons and sensitivity to longwave radiation, *J. Atmos. Sci.*, *50*, 673–690, 1993.

Trier, S. B., D. B. Parsons, and J. H. E. Clark, Environment and evolution of a cold-frontal mesoscale convective system, *Mon. Weather Rev.*, *119*, 2429–2455, 1991.

Trier, S. B., W. C. Skamarock, M. A. LeMone, D. B. Parsons, and D. P. Peterson, Structure and evolution of the 22 February 1993 TOGA COARE squall line: Numerical simulations, *J. Atmos. Sci.*, *53*, 2861–2886, 1996.

Wang, Y., W.-K. Tao, and J. Simpson, The impact of ocean surface fluxes on a TOGA COARE convective system, *Mon. Weather Rev.*, *124*, 2753–2763, 1996.

Wang, Y., D. J. Jacob, and J. A. Logan, Global simulation of tropospheric O_3-NO_x-hydrocarbon chemistry, 1, Model formulation, *J. Geophys. Res.*, *103*, 10,713–10,726, 1998.

Wang, Y.-J., A. W. DeSilva, G. C. Goldenbaum, and R. Dickerson, Nitric oxide production by simulated lightning: Dependence on current, energy, and pressure, *J. Geophys. Res.*, *103*, 19,149–19,159, 1998.

Weber, M. R., R. Boldi, P. Laroche, P. Krehbiel, and X. Shao, Use of high resolution lightning detection and localization sensors for hazardous aviation weather nowcasting, Paper presented at 17th Conference on Severe Local Storms, Am. Meteorol. Soc., St. Louis, Mo., 1993.

Williams, E. R., Large-scale charge separation in thunderstorms, *J. Geophys. Res.*, *90*, 6013–6025, 1985.

Zhang, D.-L., K. Gao, and D. B. Parsons, Numerical simulations of an intense squall line during 10–11 June 1985 PRE-STORM, 1, Model verification, *Mon. Weather Rev.*, *117*, 960–994, 1989.

J.-F. Muller, Belgian Institute for Space Aeronomy, 3, avenue Circulaire, B-1180 Brussels, Belgium. (e-mail: Jean-Francois.Muller@bira-iasb.oma.be)

K. E. Pickering, Joint Center for Earth System Science, Department of Meteorology, University of Maryland, College Park, MD 20742. (e-mail: pickerin@atmos.umd.edu)

C. Price, Department of Geophysics and Planetary Science, Tel-Aviv University, Ramat Aviv 69978, Israel. (e-mail: cprice@flash.tau.ac.il)

W.-K. Tao, NASA Goddard Space Flight Center, Code 912, Greenbelt, MD 20771. (e-mail: tao@agnes.gsfc.nasa.gov)

Y. Wang, SSAI, NASA Goddard Space Flight Center, Code 912, Greenbelt, MD 20771. (e-mail: wang@carmen.gsfc.nasa.gov)

(Received February 16, 1998; revised August 3, 1998;
accepted August 10, 1998.)